C. Hariharan* and M. Govardhan

Effect of Inlet Clearance on the Aerodynamic Performance of a Centrifugal Blower

DOI 10.1515/tjj-2015-0026
Received June 8, 2015; accepted June 17, 2015

Abstract: The present work reports the effect of inlet clearance on the performance of a centrifugal blower, with parallel wall volute, over its full operating range. For a particular impeller configuration, four volutes based on constant angular momentum principle, have been designed and analysed numerically for varying inlet clearances ranging from 0 mm (ideal clearance) to 5 mm. The computational methodology is validated using experimental data. The results indicate that as the clearance increases, the impeller performance in terms of both static and total pressure rise deteriorate. Further, the stage performances deteriorate in terms of efficiency and specific work for all mass flow rates. However, the performance of volute improves at lower mass flow rates compared to the Best Efficiency Point (BEP). A set of correlations have been developed to predict the change in stage performance as a function of clearance ratio. The non-dimensional values of change in specific work, isentropic efficiency and static pressure are found to be same irrespective of the shape of the volute.

Keywords: centrifugal blower, inlet clearance, parallel wall volute, performance, loss correlation

Introduction

A centrifugal blower essentially consists of volute and inlet duct, which are stationary components, and an impeller, which is a rotating component. There are two commonly known clearances, namely (a) tip clearance which is the clearance between impeller blades and the stationary shroud, and (b) inlet clearance which is the radial clearance between inlet duct and impeller. The inlet clearance is prone to increase during (a) commissioning; (b) due to manufacturing error and assembly tolerance and, (c) during operation due to wear and tear. Thus, the actual inlet clearance will be different from the design clearance. In general, closed impellers have no tip clearance between the blades and the shroud, there by the clearance losses are presumed to be zero. However, Lee [1] reported that there is considerable drop in performance up to 5% in a centrifugal blower with double volute and closed impeller, as the inlet clearance increases. He also highlighted that the impact of the gap on the impeller performance is much less compared to the volute performance. This suggests that the performance of a closed impeller with different volute configuration may be affected by inlet clearance. Centrifugal blowers with parallel wall volute and closed impellers are most preferred type, because of their low manufacturing cost and high pressure raise per stage. While designing such machines, there is hardly any systematic procedure or reliable correlations available, in open literature, for predicting the inlet clearance loss. Thus, there is a need to investigate the effects of increased clearance on performance of centrifugal blower with parallel wall volute. The correlations available for tip clearance are predominantly based on experiments [2–4]. Also the effect of tip clearance cannot be generalized, as it varies with machine configuration. Engin et al. [3] explored the effect of tip clearance in centrifugal pumps. Their correlation predicts the head loss with an absolute error less than 15%, for a range of tip clearance ratio. Eum et al. [4] developed a set of correlations for reduction in head and efficiency using nominal tip clearance ratio. Using the entropy generation, they presented the loss profile at impeller exit and reported that smaller tip clearances reduce the secondary flow in impeller. Ahmadbadi et al. [5] performed numerical simulation and found that by increasing the tip clearance from 0 to 1mm reduces the efficiency by 20% of a turbo-charger. Rajakumar et al. [6] studied the effect of tip clearance in high pressure mixed flow compressor. They noticed that increase in clearance resulted in considerable drop in pressure raise and peak efficiency, as well as, reduced choke and surge mass flow. Hong et al. [7] reported the effect of tip clearance on downstream components (e.g. vaneless diffuser) and developed a

***Corresponding author: C. Hariharan,** Department of Mechanical Engineering, Thermal Turbomachines Laboratory, Indian Institute of Technology Madras, Chennai – 600036, India, E-mail: hari_pblr@yahoo.co.in
M. Govardhan, Department of Mechanical Engineering, Thermal Turbomachines Laboratory, Indian Institute of Technology Madras, Chennai – 600036, India, E-mail: gova@iitm.ac.in

one dimensional correlation between drop in performance and tip clearance width ratio. Ayder et al. [8] carried an experimental study of the flow in an elliptical volute. Herein, they presented the pressure distributions along the periphery of the volute. They also developed a one-dimensional loss prediction correlation. Several investigators [9–11] performed numerical analysis effect of tip clearance on the performance of centrifugal blower. However, there is a scarcity of studies reported on the detailed influence of inlet clearance especially on parallel wall volutes. Hariharan and Govardhan [12] numerically simulated the flow inside the parallel wall volute for different area ratios at design and off design conditions and presented the effect of increase in cross sectional area of the volute on the performance of the blower. In another study [13], they numerically simulated the flow in a centrifugal blower with and without clearance and presented the over-prediction of performance due to omission of inlet clearance in numerical simulations. Compared to other aerodynamic and geometrical parameters in centrifugal blowers, the effect of inlet clearance is generally ignored in earlier studies, because of its negligible effect on overall performance. This may be acceptable for other centrifugal machines, but in centrifugal blowers with parallel wall volute, the clearance flow enters directly from the volute into the impeller exposing it to high pressure and high energy fluid. Thus, the present work is an attempt to investigate the effect of inlet clearance on the performance of a typical industrial centrifugal blower with parallel wall volute for varying width ratios, both at stage and component level.

Design and analysis

Blower configuration and design parameters

The radial clearance between the suction duct and the impeller is maintained at 1 mm 3 mm and 5 mm representing 0.6%, 1.8% and 3% of the inlet area, respectively. Four volutes (R 5.0, R4.0, R 3.5 and R 3.0. R 5.0 represent the ratio of volute width to impeller width = 5.0) are designed based on constant angular momentum principle as shown in Figure 1(a) Parallel wall volutes with width ratios (the ratio between the volute width and the impeller exit width) of 5.0, 4.0, 3.5 and 3.0 are used, as per the industrial standards towards cost effectiveness. The tongue clearance (radial distance from rotational axis) as well as the tongue position (32° with respect to outlet) are maintained constant for all volutes. The detailed design and geometrical values of the blower configuration are presented in Table 1. As shown in Figure 1(b) entire

Table 1: Design and geometrical values of blower.

Impeller Inlet Diameter	0.6 m
Impeller Exit Diameter	1.3 m
Inlet Blade angle	31°
Exit Blade angle	48°
Number of blades	15
Design specific work	24,000 m^2/s^2
Design mass flow rate	28.5 kg/s
Operating rage	20–31.5 kg/s
Speed	3,000 rpm

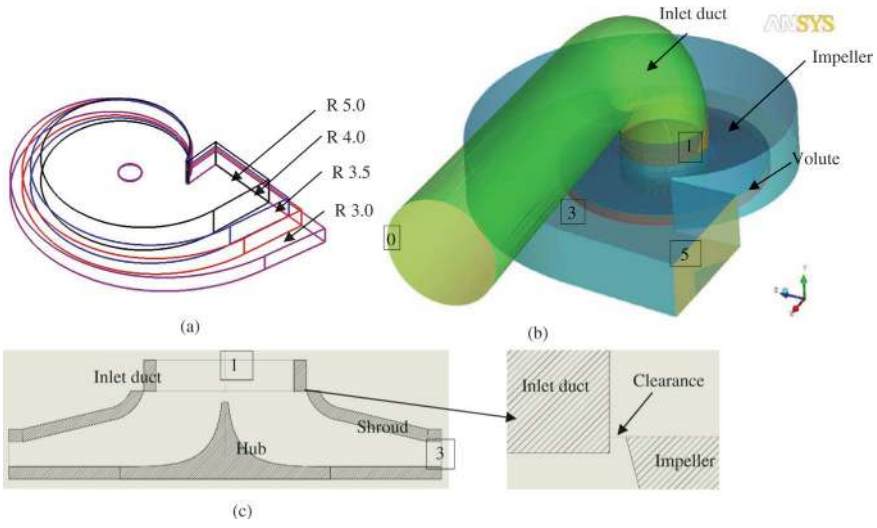

Figure 1: (a) 3-D View of R 3.0, R 3.5, R 4.0 and R 5.0 volutes (b) 3-D view of fan assembly for R 5.0 volute with clearance of τ_1 (1 mm) (c) Meridional view of impeller.

impeller and the suction duct are placed inside the volute and Figure 1(c) shows the enlarge view of clearance gap. It can be noticed that the suction duct extends into the impeller by 3 mm. The various stations are marked in Figure 1.

CFD methodology

In the present study continuity, energy and Reynolds averaged Navier-Stokes equations with k-ε turbulence model are discretised and solved iteratively using ANSYS CFX 14. A second order scheme is utilized for spatial discretization. A total number of 80 simulations are carried out both at design and off-design conditions for five mass flow rates ($m/m_d = 0.7–1.1$), three clearances (1 mm, 3 mm and 5 mm) and normalized with ideal clearance (zero clearance) for four volutes ratio 5, 4, 3.5 and 3. Due to the asymmetric nature of volute geometry and the 3-D nature of flow inside volute, the computational domain consists of all the fluid regions with in the control volume. Air is chosen as working fluid. Due to compressible nature of flow an ideal gas assumption is made. The total pressure at inlet and mass flow at outlet boundary conditions are imposed. The inlet total pressure and temperature are equal to the atmospheric pressure and 300 K. This is a reasonable and practical condition because the inlet is placed in the suction duct, which is open to the atmosphere. An outlet mass flow boundary is maintained at the volute outlet, as throttle valve is being used at the exit of volute to control mass flow rates. All the walls are assumed as smooth and adiabatic. The transfer of information between rotating and stationary domain is employed by frozen rotor approach. Simulation is continued till steady state values of flow parameters like total pressure at outlet, shaft input torque and mass flow at inlet are attained. The RMS convergence criteria have been fixed as $1\ E^{-5}$. The average CPU time for a single simulation is 150 h in a 32 GB RAM and 8 processor workstation.

The grid independence is examined based on Richardson grid independence study [14] and the results are furnished in Table 2. CGI index (0.25%) shows the grid convergence is attained for current configuration. Further increase in number of elements had negligible effect on the results. Thus, the final hexahedral mesh (96,04,524 elements) consists of 5.5, 4.5 and 0.15 million nodes for impeller, volute and inlet duct, respectively.

Table 2: Richardson grid independence study.

No of Elements N_1, N_2, N_3	96,04,524, 41,96,409, 21,09,898
Grid refinement factor (r_{21})	1.32
Grid refinement factor (r_{32})	1.31
Critical variable value for grid 1 (φ_1)	18,160.1
Critical variable value for grid 2 (φ_2)	18,244.83
Critical variable value for grid 3 (φ_3)	18,522.73
Apparent order (P)	4.45
Extrapolated values (φ_{ext}^{21})	18,125
Approximate relative error (e_a^{21})	0.46%
Extrapolated relative error (e_{ext}^{21})	0.19%
Fine grid convergence index (CGI_{fine}^{21})	0.24%

Validation

The computational methodology is validated using the test rig data available at Thermal Turbomachinery Laboratory in the Indian Institute of Technology Madras. The test rig consist of centrifugal blower with parallel wall volute (design and test rig has almost same non-dimensional shape number). Details regarding test rig are available in Ref. [15]. The CFD results are compared both in terms of global and local values. Figures 2(a) show the stage isentropic specific work and efficiency for different flow rates. The results show close comparison between the experimental and computed values. Maximum difference in specific work of 1.5% is noticed at 0.8 m^3/s; the experimentally measured isentropic efficiency is 2.7% less than the CFD values at almost all volume flow rates except at lower flow rate, where the difference is 5.6%. This deviation could be attributed to a slight fluctuation in the blower speed during the tests, while simulations are calculated at a constant speed. Figure 2(b) depicts static pressure at the exit of impeller across the volute width at 90^o from tongue. It is evident the computation and experimental results are in good agreement.

Results and discussion

The results obtained from the computations are presented for individual component, as well as for the entire stage. The inlet clearances are represented in terms of the inlet clearance ratio (τ) as follows:

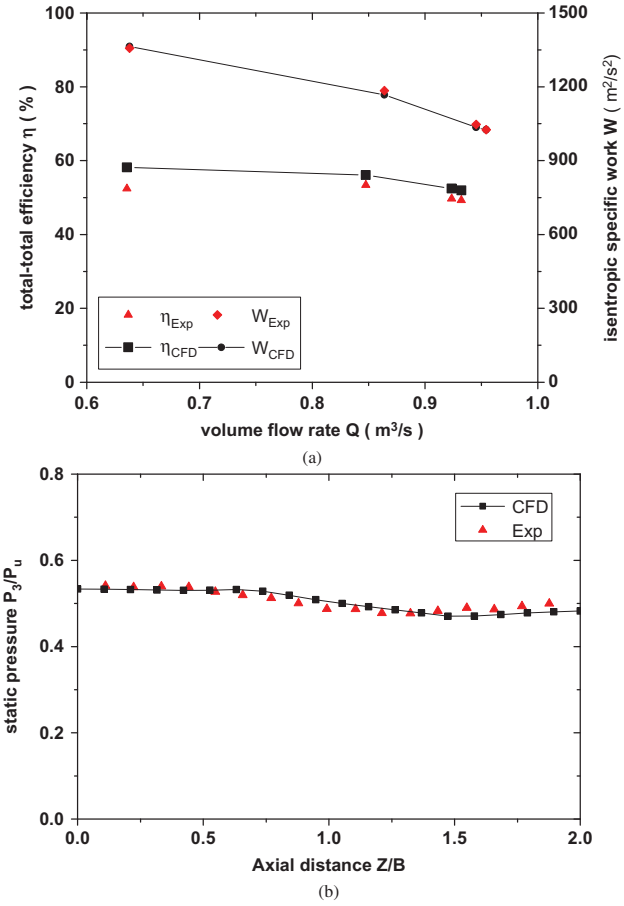

Figure 2: (a) Specific work and isentropic efficiency (b) Static pressure across the volute width.

$$\tau = \frac{\text{Inlet clearance}}{\text{Inlet radius}} \times 100 \tag{1}$$

Thus, τ_0, τ_1, τ_2 and τ_3 represents inlet clearance ratio for an inlet clearance of 0 mm, 1 mm, 3 mm and 5 mm, respectively.

Stage performance

Specific work and efficiency

The change in the isentropic specific work due to increase in inlet clearance is plotted in Figure 3 for different mass flow rates and volute shapes. The values are plotted relative to those for ideal clearance of 0 mm (τ_0). To isolate the effect of clearance the change in values are non-dimensioned by ideal clearance values [5]. The percentage change in isentropic specific work can be represented as.

$$C_w = \left(\frac{W - W_{\tau_0}}{W_{\tau_0}}\right) \times 100 \tag{2}$$

$$\text{Where, } W = \left(\left(\frac{P_{05}}{P_{00}}\right)^{\frac{(\gamma-1)}{\gamma}} - 1\right) \times C_p \times T_{00} \tag{3}$$

P_{05} is the total pressure at exit of the stage,

P_{00} and T_{00} are the total pressure and temperature at the inlet to the stage.

The change in specific work for all the volutes follows the same trend for the corresponding clearance. At design ($m/m_d = 1.0$) and higher mass flow rates for τ_2 and τ_3 all volutes show drop in specific work. The drop keeps reducing towards lower mass flow rates. At lowest mass flow rate ($m/m_d = 0.7$), an increase in the clearance shows positive effect on specific work. Regardless of volute, there is an increase in specific work especially for τ_1 clearance, where the mass flow rate is less than design mass flow rate. The slope of the C_W curve keeps increasing with increase in clearance indicating that higher the clearance higher the drop in specific work.

The change in isentropic stage efficiency (total-total) is plotted in Figure 3. The percentage change in isentropic stage efficiency can be calculated using eq. (4).

$$C_\eta = \left(\frac{\eta - \eta_{\tau_0}}{\eta_{\tau_0}}\right) \times 100 \tag{4}$$

The efficiency follows the same trend as noticed earlier for specific work. However, the magnitude of change is almost twice the magnitude of specific work. The reason being the efficiency is a function of input power and specific work. For increased clearance, the specific work is reduced but the input power is not proportionately changed. The clearance has higher impact on efficiency compared to the specific work. The blower performance is almost constant at low clearance, whereas it is more sensitive to mass flow rates at other clearance gaps.

Correlations

Many researchers [2–4, 7] suggested the change in performance of centrifugal machine due to tip clearance is directionally proportional to nominal clearance ratio. The present computational results exhibit the same trend for inlet clearance effects on impeller and downstream components. Thus, the change in specific work depends on clearance area and shape of the blade. Clearance area linearly varies with clearance gap when $\tau << 1$. To account for impeller shape, a non-dimensional variable

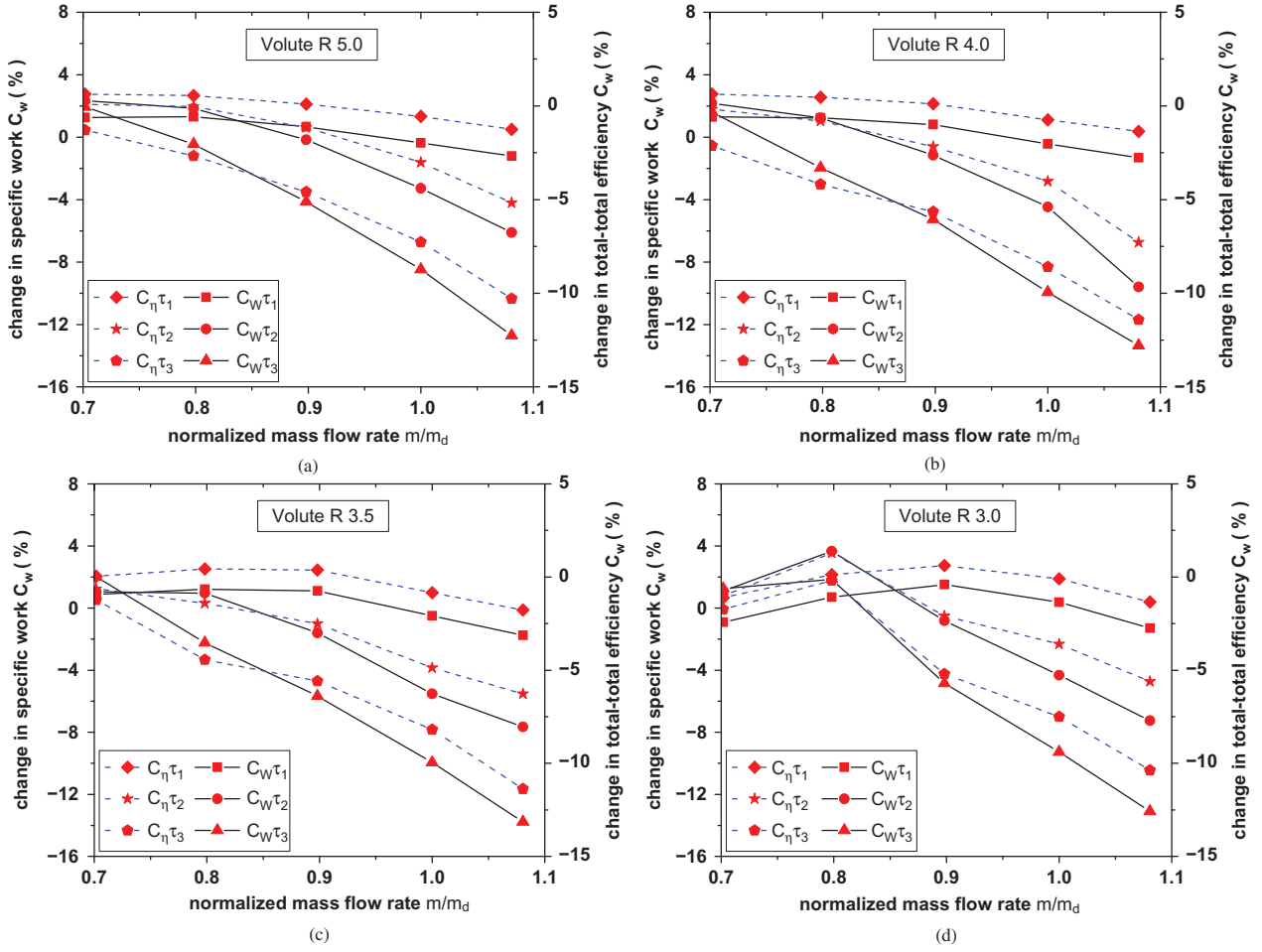

Figure 3: Change in isentropic specific work and change in isentropic efficiency of the stage with mass flow rate for different volutes: (a) R 5.0 (b) R 4.0 (C) R 3.5 (d) R 3.0.

namely, shape number as described in eq. (5) has been employed. The specific work is inversely proportional to shape number.

$$N_s = \frac{n \times \sqrt{Q}}{W^{\frac{3}{4}}} \tag{5}$$

The following correlations have been developed in terms of clearance ratio and shape number.

$$C_w = \frac{\tau}{N_s^{\left(\frac{3}{4}\right)}} \tag{6}$$

$$C_\eta = \frac{\tau}{N_s^{\left(\frac{3}{4}\right)}} \tag{7}$$

In Table 3 the comparison of loss in specific work and efficiency at design points are presented. Correlations found to predict values closer to the CFD values for all cases with a maximum deviation of 20% for specific work and efficiency, except lower clearance. To make them more generic, the other variables like volute ratio, impeller blade angles and the like need to be considered, which can eventually make the correlations nonlinear and more complex to solve. Hence these simplified correlations have been developed in order to assist the designers at primary design stage to predict the change in the isentropic specific work

Table 3: Loss in specific work and efficiency at design mass flow rate.

		CFD				Predicted
		R 5.0	R 4.0	R 3.5	R 3.0	
C_w (%)	τ_1	−0.37	−0.44	−0.50	0.38	−1.59
	τ_2	−3.28	−4.47	−5.52	−4.32	−4.78
	τ_3	−8.47	−9.94	−9.96	−9.28	−7.97
C_η (%)	τ_1	−0.56	−0.75	−0.84	−0.10	−1.59
	τ_2	−3.02	−4.02	−4.87	−3.60	−4.78
	τ_3	−7.26	−8.59	−8.20	−7.50	−7.97

and efficiency at design mass flow for different combination of volute width ratios and inlet clearances.

Return mass flow rate

The return mass flow entering from the volute to the impeller inlet for different mass flow rates is plotted in Figure 4. Return mass flow is almost constant for low clearance values and is independent of mass flow rate and volute shape. For higher clearance gaps, the return mass flow slightly increases with decrease in mass flow rate. The factors deciding the return flow are the pressure difference and area of clearance. In the stage with increased clearance, impeller handles inlet mass flow rate as well as the mass flow from the clearance. This changes the operating condition of the impeller with consequent change in the performance.

Impeller performance

Total and static pressure

Figure 5 shows the change in total pressure at the exit of the impeller for different mass flow rates. The percentage change in total pressure can be obtained using eq. (8).

$$C_{\Delta P_{03}} = \left(\frac{P_{03} - P_{03\tau_0}}{P_{03\tau_0}}\right) \times 100 \tag{8}$$

The total pressure at inlet to the impeller is constant for all mass flow rates and volutes. The change in total pressure at the exit of the impeller represents the work done by impeller. The increased clearance shows drop in total pressure irrespective of clearance gap, volute shape and mass flow rates. The change in total pressure

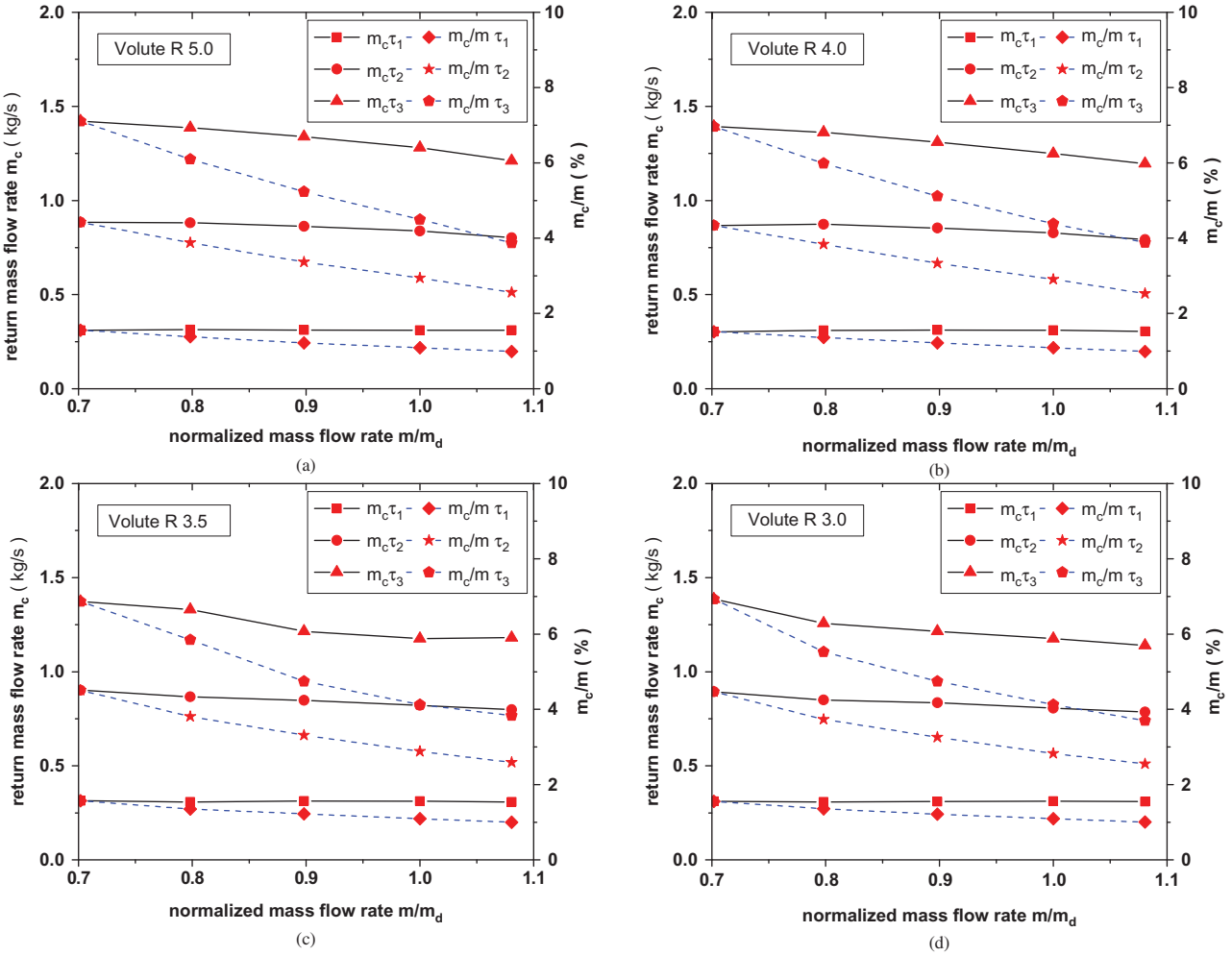

Figure 4: Return mass flow rate with mass flow rate for different volutes: (a) R 5.0 (b) R 4.0 (c) R 3.5 (d) R 3.0.

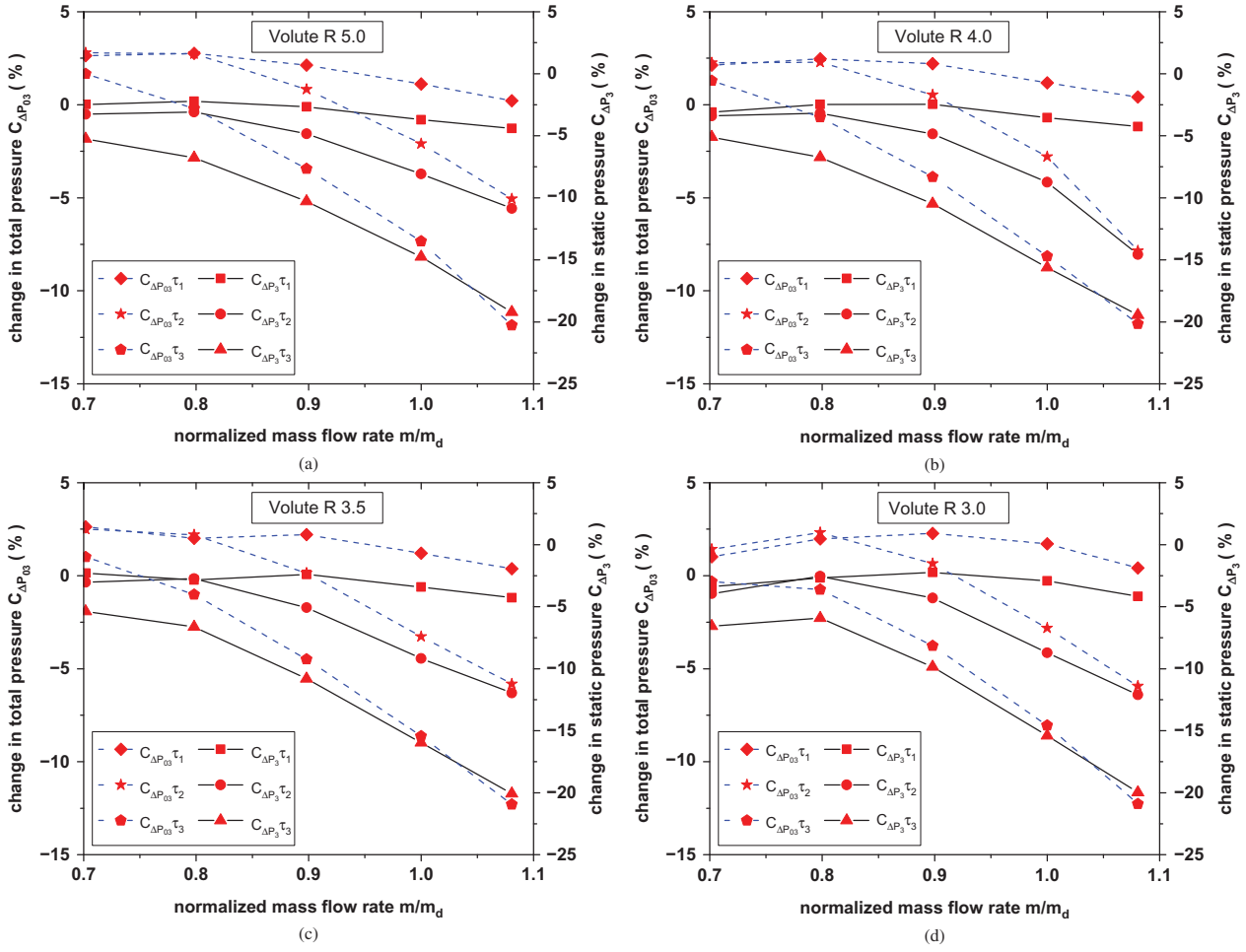

Figure 5: Change in total pressure and static pressure at impeller exit with mass flow rate for different volutes: (a) R 5.0 (b) R 4.0 (c) R 3.5 (d) R 3.0.

also follows the same trend as other variables. The drop is high at higher mass flow rates and keeps decreasing towards the lower mass flow rates. Further it is inferred that higher the clearance higher is the drop.

Figure 5 shows the change in static pressure at the impeller exit. Dynamic pressure (total pressure – static Pressure) is the energy entering the volute for pressure recovery. In general, higher dynamic pressure leads to higher losses. Hence, the static pressure should be high enough to reduce the dynamic pressure, thereby the losses. It is observed from Figure 8 that increase in clearance results in drop in static pressure and the change is approximately 2 times the change in total pressure. The percentage change in static pressure is calculated using eq. (9).

$$C_{\Delta P_3} = \left(\frac{P_3 - P_{3\tau_0}}{P_{3\tau_0}}\right) \times 100 \qquad (9)$$

Flow field inside the impeller for R 5.0 volute

To understand the loss mechanism with increase in clearance, the detailed flow field in the impeller is considered. In the present paper, R 5.0 volute parameters for different clearance gaps are presented in terms of pressure, velocity and flow angles at the inlet and exit of the impeller. The main impact of increased clearance in the impeller is the interaction between high energy and high velocity fluid from volute entering the impeller inlet with the low energy fluid coming from the inlet duct and taking 90^0, Kim et al. [16]. This leads to incidence angle at design point itself, which should not happen for ideal situation.

Contours of flow angle

Figures 6 show the contours of flow angle at impeller inlet for $m/m_d = 1.1$. The contours are plotted closer to leading

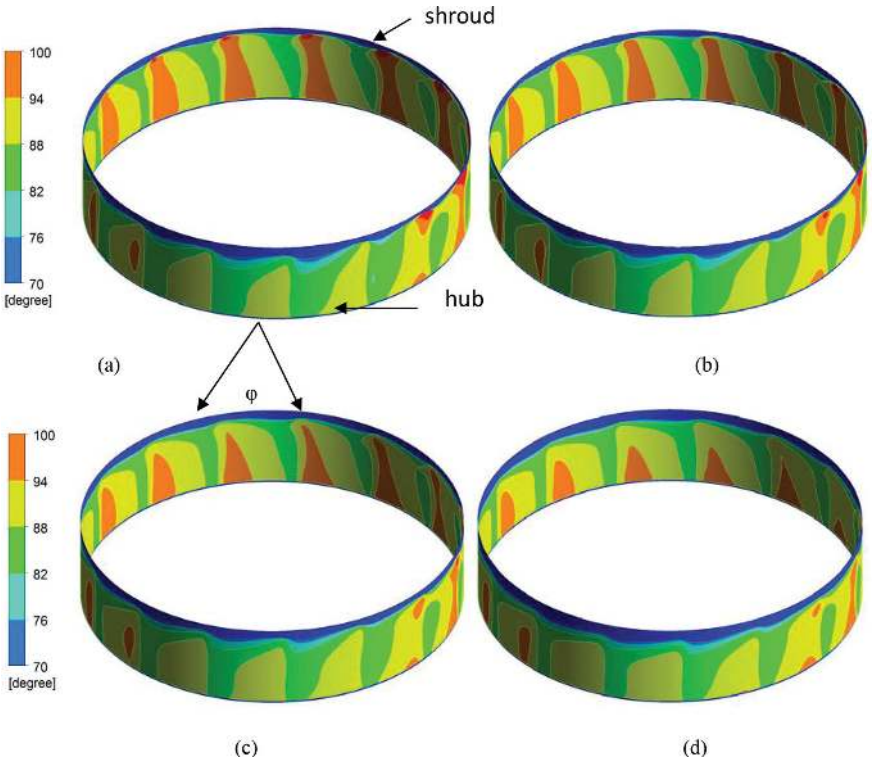

Figure 6: Flow angle variation at impeller inlet for m/md = 1.1 of R 5.0 volute (a) τ_0, (b) τ_1, (c) τ_2, (d) τ_3.

edge of the impeller along the peripheral direction for full span, from hub to shroud. It is noticed that there is a variation in flow angle along the peripheral and spanwise directions for all clearances, and the variation increases gradually with the clearance value. For instance, (as indicated in Figure 6) in peripheral direction, the flow angle disturbance for a particular blade to blade sector (φ) increases with increase in clearance. Besides, the variation in flow angle is quite evident at tongue region for various clearances. Similarly there is a noticeable non-uniformity in the flow angle across the spanwise direction, especially closer to the shroud, which is more evident for higher clearance. The mass weighted average flow angle is more or less from the design value of 90^0. For τ_2 and τ_3 the results show more uniformity in angles, which are closer to design value, compared to τ_1 and ideal clearance cases. Because high energy clearance flow mixes with low energy flow from inlet leads to more homogeneous flow.

Contours of relative velocity

Figures 7 and 8 show the relative velocity contours in impeller at meridional plane for $m/m_d = 0.7$ and 1.1,

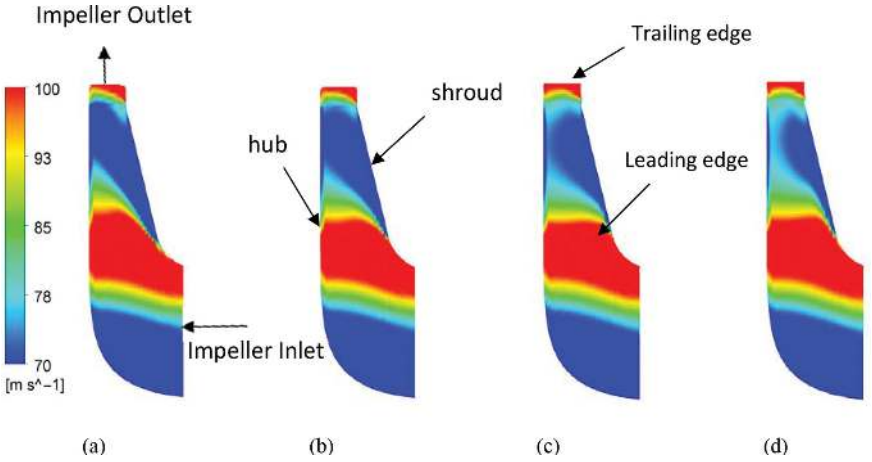

Figure 7: Relative velocity in the meridional plane of the impeller for m/md = 0.7 of R 5.0 volute a) τ_0, (b) τ_1, (c) τ_2, (d) τ_3.

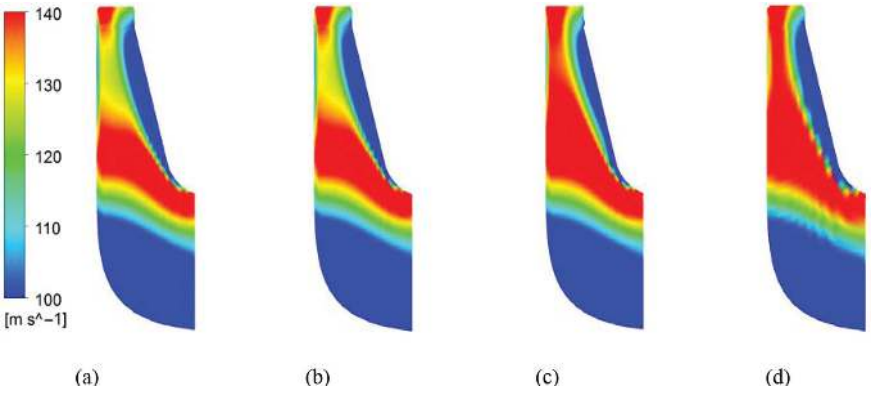

Figure 8: Relative velocity in the meridional plane of impeller for m/md = 1.1 of R 5.0 volute a) τ_0, (b) τ_1, (c) τ_2, (d) τ_3.

respectively. The meridional passage is divergent hence the flow decelerates along the path. However, the spanwise disturbance is still continuing from the leading to the trailing edge of the impeller. Closer to the trailing edge, all clearances show noticeable variation in velocity along the span, whereas closer to hub, the velocity is maximum and keeps decreasing towards the shroud. A higher clearance results in increase in velocity along the span and the increment is directly proportional to the clearance. The velocity at the impeller exit is more or less uniform along the span compared to the lower clearance gaps.

Because of inlet clearance, flow from the impeller blades is disturbed in span wise and circumferential directions, position of separation point changes closer to the trailing edge of the impeller blade. Due to these change in incidence, the pressure developed by the impeller also varies. Figures 9 show the variation of static pressure at the exit of the impeller in the

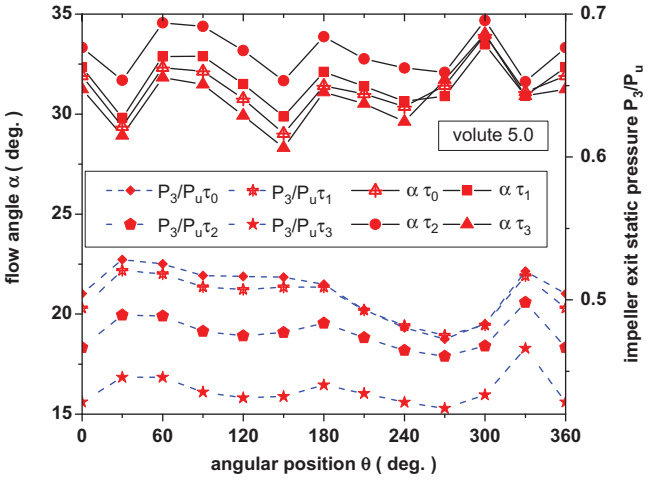

Figure 9: Variation of static pressure and flow angle at the exit of the impeller along the circumferential direction for $m/m_d = 1.0$ of R 5.0 volute.

circumferential direction for $m/m_d = 1.0$. At design point, the increase in the clearance reduces the static pressure developed in the impeller. The spanwise disturbed flow along the meridional path leads to additional loss reducing the static pressure developed at the impeller exit. All along the sector it follows the same trend for all clearances.

The work done by the impeller depends on velocity and relative flow angle at the exit of impeller for zero swirl inlet. Figure 9 show the relative flow angle at the exit of the impeller along the circumferential direction for $m/m_d = 1.0$. At design point, the increased clearance results in increase in flow angle (the change in flow angle from inlet to exit of the impeller is one of the key parameters for work done by impeller); the same is reflected in total pressure. The interaction between the flow coming from the volute and the impeller leads to variation in the flow angle along the circumferential direction. The variation is less for high and medium clearances compared to low clearance, because of the additional mixing of flow due to spanwise disturbance.

The main effect of clearance is to change the flow separation on the suction surface of the impeller blade. The reduction in the impeller performance is quantified by the change in flow angle and change in total pressure at the impeller exit. To understand qualitatively (see Figure 10), the velocity streamlines are plotted from the impeller inlet to exit of the impeller for $m/m_d = 0.7$. At $m/m_d = 0.7$, flow separation is present for all clearance gaps, and is more predominant in low clearance cases. At higher clearance gaps, almost five times more high energy leakage fluid mixes with low energy main fluid and thus reducing the flow separation especially closer to the trailing edge of the impeller blade. The spanwise disturbance aids in delaying the flow separation on suction surface of the blade, hence the static pressure developed at the exit of the impeller is increased.

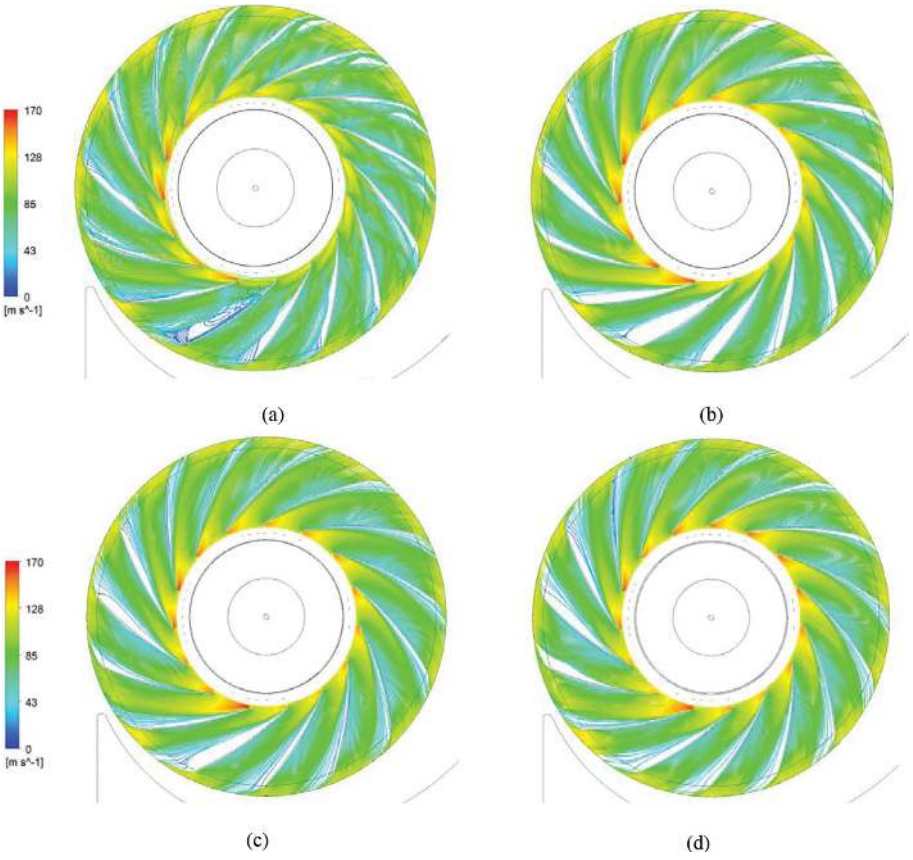

Figure 10: Velocity stream lines from the impeller inlet to the impeller exit for m/md = 0.7 of R 5.0 volute a) τ_0, (b) τ_1, (c) τ_2, (d) τ_3.

Volute performance

Volute is designed based on constant angular momentum principle. One of the assumptions is that the flow always follows logarithmic spiral path. But due to interaction between the flow coming from impeller with the volute flow, primarily at off design conditions, the flow angle varies from design value of $\alpha_3 = 32^o$. The spanwise variation of flow angle and velocity leads to additional loss in volute.

Pressure recovery and loss in the volute

Pressure recovery coefficient (C_p) is defined as the ratio between the static pressure recovered in the volute to the dynamic pressure at the impeller exit.

$$C_p = \frac{P_5 - P_3}{P_{03} - P_3} \tag{10}$$

The variation of pressure recovery coefficient with mass flow rate is shown in Figure 11. The increase in clearance reduces the pressure recovery at $m/m_d = 1.0$ and 1.1. The spanwise disturbance induced due to clearance flow leads to additional loss and results in reduced pressure recovery. At lower mass flow rates (below design value), it has positive effect which means higher the clearance higher the pressure recovery, this is the result of available dynamic pressure at impeller exit being directly proportional to clearance. For higher ratio volutes, the slope of change in pressure recovery is slightly high compared to lower ratio volutes. At $m/m_d = 0.7$, the increase in pressure recovery values of R 5.0 volute are 3%, 8% and 11%, respectively, for τ_1, τ_2 and τ_3.

Loss coefficient (ω), is defined as the ratio between the total pressure losses in the volute to the dynamic pressure at the impeller exit.

$$C_\omega = \frac{P_{03} - P_{05}}{P_{03} - P_3} \tag{11}$$

Figure 11 shows the variation of loss coefficient with different mass flow rates. The loss coefficient is inversely proportional to pressure recovery coefficient. At design point, all clearance gaps have almost same loss coefficient. Loss increases with clearance at higher mass flow rates whereas, the loss decreases with increase in clearance at lower mass flow rates. More uniform flow and the reduction in deviation angle result in reduced loss. The

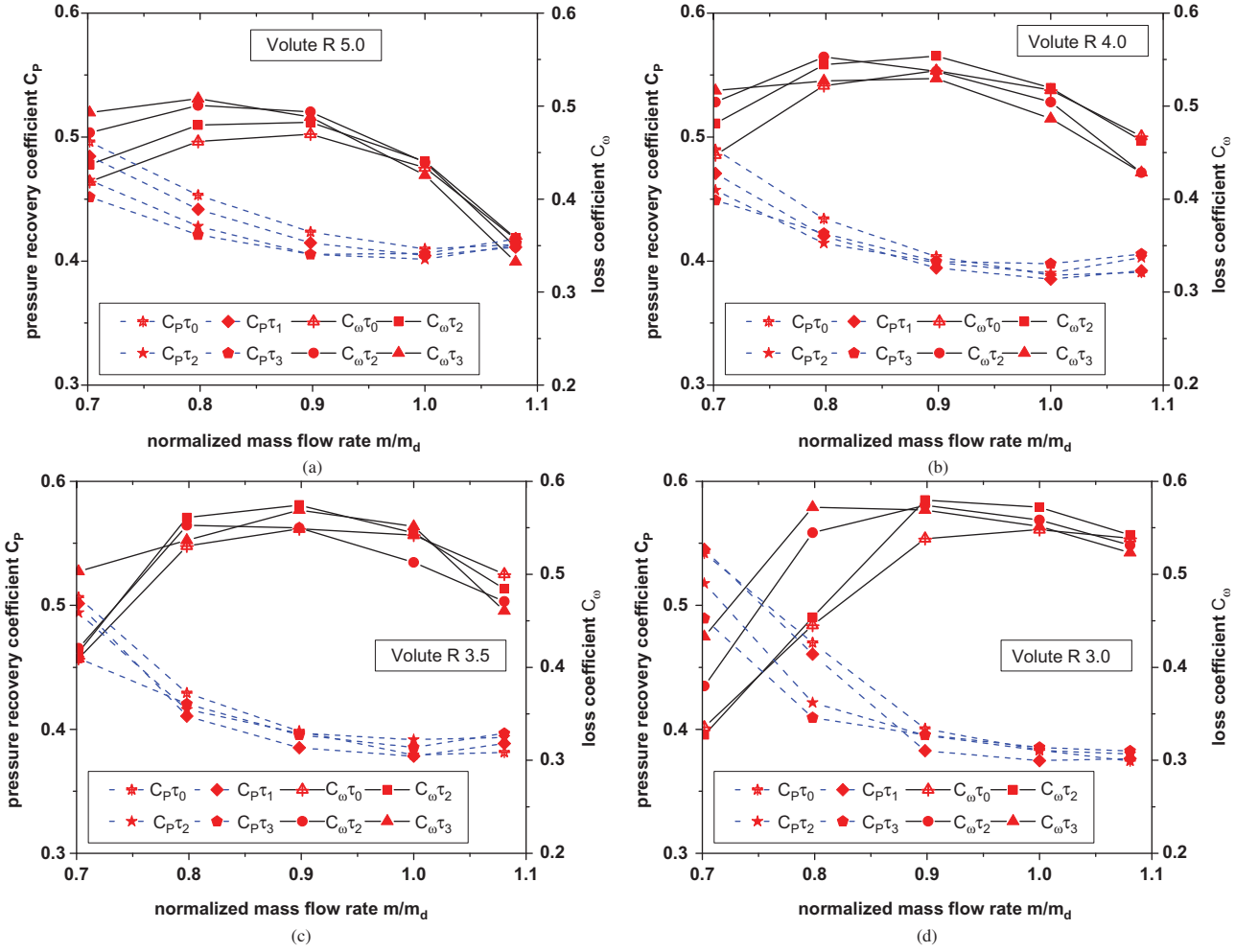

Figure 11: Variation of pressure recovery and loss coefficient with mass flow rate for different volutes (a) R 5.0 (b) R 4.0 (C) R 3.5 (d) R 3.0.

slope of loss coefficient vs (m/m_d) curve increases with increase in clearance area. At $m/m_d = 0.7$, the decrease in loss coefficient values for R5.0 volute are 3.5%, 10% and 15%, respectively, for τ_1, τ_2 and τ_3.

Static pressure

The change in static pressure at the volute exit due to the clearance is computed as:

$$C_{\Delta P_5} = \left(\frac{P_5 - P_{5\tau_0}}{P_{5\tau_0}}\right) \times 100 \qquad (12)$$

Figure 12 shows the change in static pressure at the exit of the volute for different mass flow rates. The ideal blower should deliver high static pressure for a given mass flow rate. Due to increased clearance, the static pressure is decreased. The change in static pressure also follows the same trend as specific work but with slightly higher magnitude. The maximum change in static pressures for τ_3 at $m/m_d = 1.0$ are 2,200, 2,600, 2,300 and 2,200 N/m^2 for R5.0, R4.0, R3.5 and R3.0, respectively.

Flow field inside the volute

To better understand the pressure recovery mechanism, the mass weighted average across the cross-section of the velocity inside the volutes is plotted at different peripheral angle. The velocity inside the volute is split into two components (i) through flow velocity (the velocity perpendicular to cross section of the volute) (ii) cross flow velocity (the velocity parallel to cross section of the volute). Through flow velocity is the main contributor for the pressure recovery. Figures 13 show the variation of through flow velocity at different cross sections of the volute for $m/m_d = 1.0$. The effect of clearance is more pronounced closer to the tongue than the throat area. Higher the clearance, higher is the velocity, which in turn

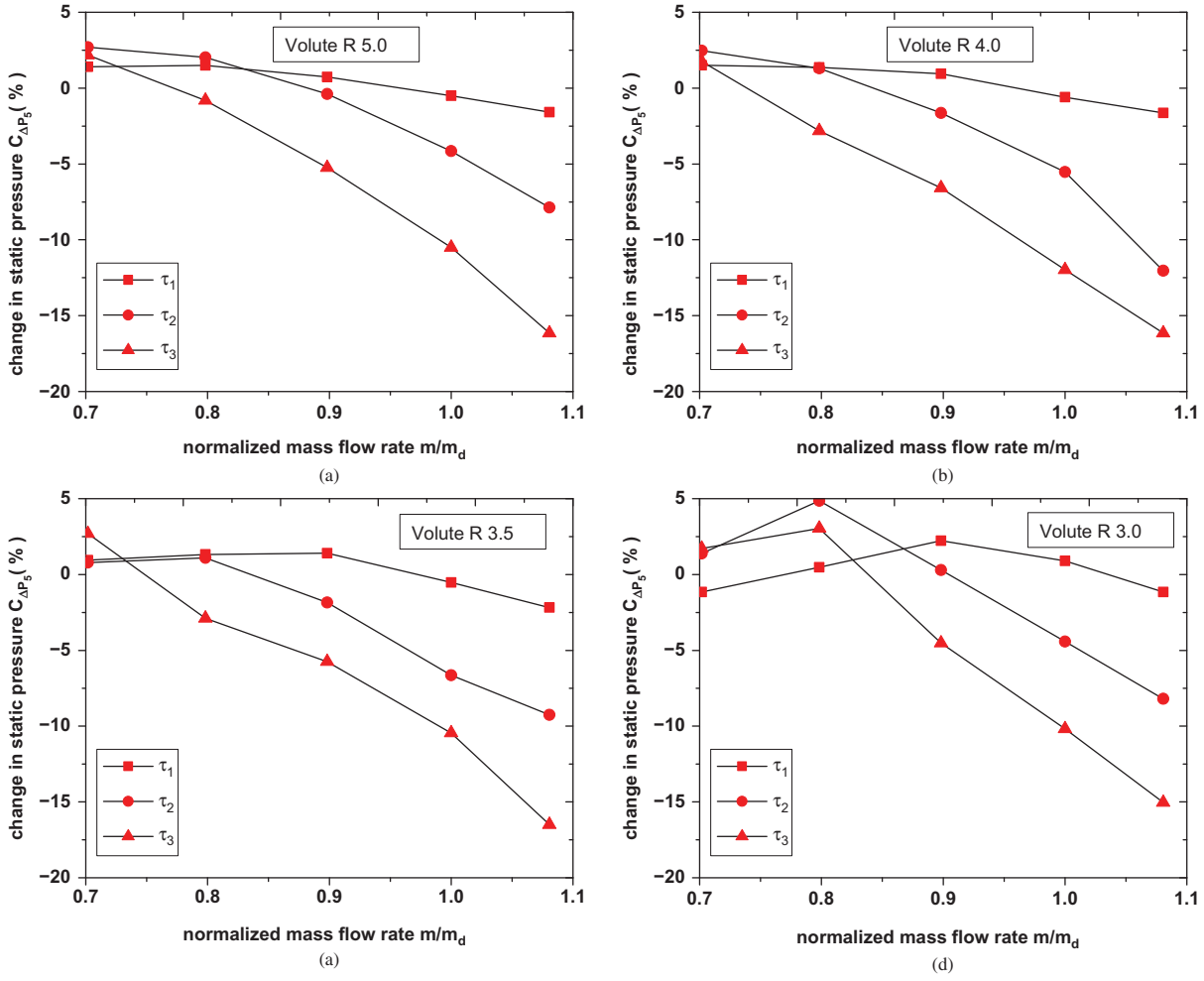

Figure 12: Change in static pressure at volute exit with mass flow rate for different volutes: (a) R 5.0 (b) R 4.0 (C) R 3.5 (d) R 3.0.

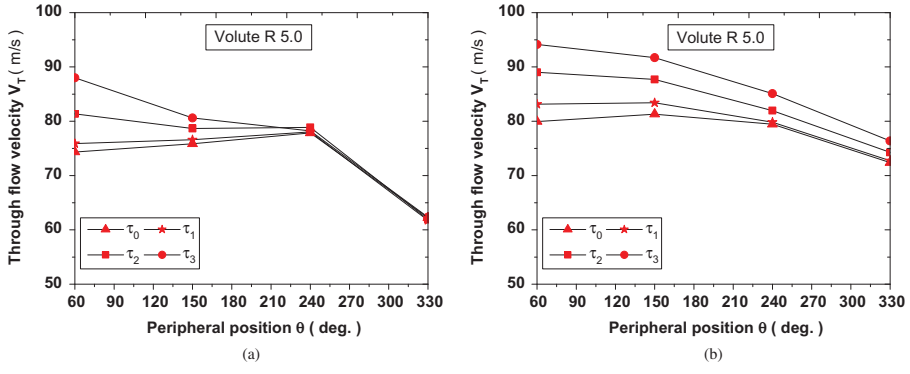

Figure 13: Through flow velocity at the cross sections of the volute along the circumferential direction (a) m/md = 0.7 and (b) m/md = 1.0.

increases the pressure recovery coefficient. For τ_3, the presence of dynamic pressure is high at the exit of impeller. At design point, the difference in values of velocity closer to tongue are 3 m/s, 9 m/s, 14 m/s for τ_1, τ_2 and τ_3, respectively. At throat, the differences in the values of velocity are 2 m/s and 4 m/s for τ_2 and τ_3, respectively.

To qualitatively understand the flow field inside the volute, streamlines along the volute are plotted for $m/m_d = 0.7$ (see Figure 14). The change in the performance of volute is due to the deviation of flow path from ideal logarithmic spiral path. At design $m/m_d = 0.7$ for higher (τ_3) clearance, the flow traverses additional

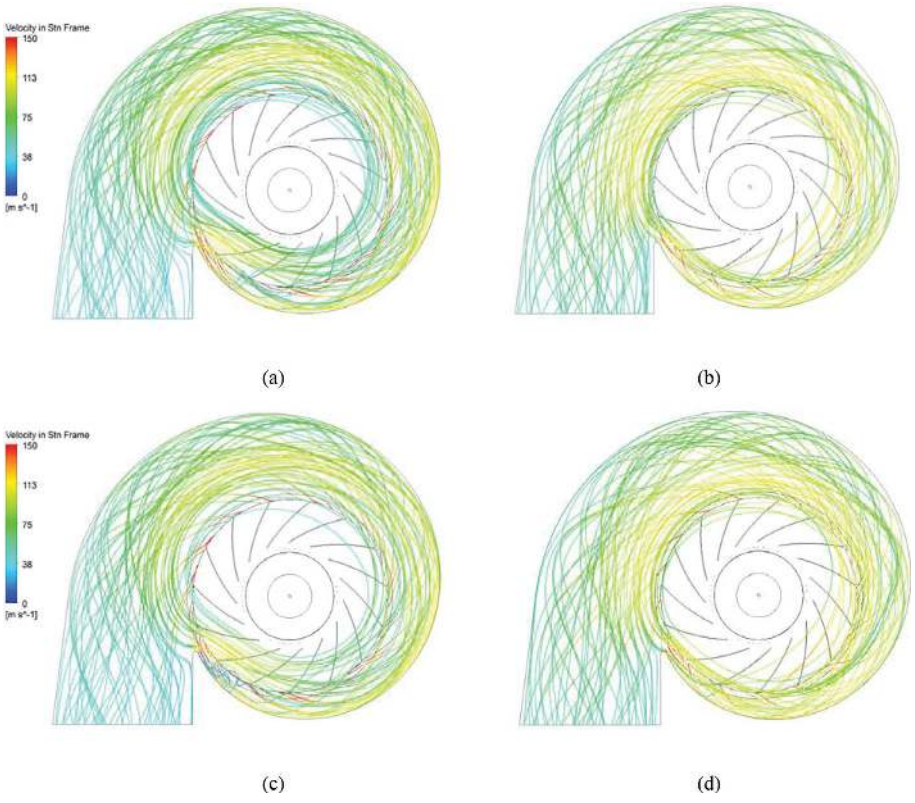

Figure 14: Velocity stream lines from the impeller exit to the volute exit for $m/m_d = 1.0$ of R 5.0 volute a) τ_0, (b) τ_1, (c) τ_2, (d) τ_3.

distance along the inlet duct, which eventually increases the volute losses. The amount of flow recirculation is increased with clearance area, which also accounts for this loss in volute. Further, all volutes show recirculation near the tongue region at the lowest mass flow rate. In ideal and low clearance gaps, the recirculating flow mixes with main flow coming from the impeller, resulting in increased losses. In higher clearance case, recirculation gets accumulated between the shroud and the top wall of the volute, and then enters the impeller, thereby reducing the loss in volute.

Conclusions

The effect of clearance between the inlet duct and the impeller for a typical industrial centrifugal blower with parallel wall volute is investigated numerically and the detailed flow physics are reported. The salient features are summarized as below.

- At component level, regardless of the volute, there is a noticeable drop in total and static pressures at the impeller exit for all mass flow rates with increased inlet clearance values. Flow is found to be more uniform at the impeller exit with increase in clearance gaps. However, at the impeller inlet, flow is more uniform only for higher mass flow rate and higher clearance gap combinations. Besides, there is a noticeable delay in flow separation on the suction side of the blade for lower mass flow rates and higher clearance combinations.
- The increase in inlet clearance has a beneficial effect in all volutes in terms of reduced loss and increased pressure recovery for almost all mass flow rates. Thus the increased through flow velocity with clearance is well justified.
- At system level, the increase in clearance reduces specific work, isentropic efficiency and static pressure at stage exit for almost all mass flow rates, except for a slightly increased value at lowest mass flow rates. This implies that the desirable effect can be achieved only at lowest mass flow rates, regardless of volute. It can be noticed that input power required is inversely proportional to the mass flow rates and clearance area up to the best efficiency point; and the effect is reversed afterwards.
- The set of correlations developed as a function of clearance ratio can assist the designers in predicting the change in specific work and efficiency during the preliminary design stage. However further work is

required to make the correlation generic, which should include other variables like volute ratio, mass flow rate and impeller blade angles.

Nomenclature

C_p	pressure recovery coefficient
m	mass flow rate (kg/s)
m_c	return mass flow rate (kg/s)
P	static pressure (N/m^2)
P_0	total pressure (N/m^2)
$C_{\Delta P3}$	change in static pressure at impeller exit (%)
$C_{\Delta P03}$	change in total pressure at impeller exit (%)
$C_{\Delta P5}$	change in static pressure at volute exit (%)
Q	volume flow rate (m^3/s)
V_T	through flow velocity (m/s)
W	isentropic specific work (m^2/s^2)
$C_{\Delta W}$	change in isentropic specific work (%)
Z/B	ratio of axial position to blade height
α	flow angle with respect to tangential direction (deg.)
η	Total to Toal isentropic efficiency of stage (%)
$C_{\Delta\eta}$	change in isentropic efficiency (%)
θ	angular position with respect to tongue (deg.)
τ	inlet clearance ratio (ratio of radial clearance to impeller inlet radius)
ρ	density (kg/m^3)
φ	angle between successive blades (deg.)
C_ω	volute loss flow coefficient

Subscripts

0	inlet of suction duct
1	exit of suction duct
2	inlet of impeller
3	exit of impeller
4	inlet to volute
5	exit of volute
d	design value

Abbreviations

B2	impeller exit width (m)
B5	volute exit width (m)
R 3.0	Ratio of volute width to impeller width = 3.0
R 3.5	Ratio of volute width to impeller width = 3.5
R 4.0	Ratio of volute width to impeller width = 4.0
R 5.0	Ratio of volute width to impeller width = 5.0
τ_0	inlet clearance ratio of 0 mm
τ_1	inlet clearance ratio of 1 mm
τ_2	inlet clearance ratio of 3 mm
τ_3	inlet clearance ratio of 5 mm

References

1. Lee YT. Impact of fan gap flow on the centrifugal impeller aerodynamics. J Fluids Eng 2010;132:91103–911031.
2. Engin T, Gur M, Scholz R. Effects of tip clearance and impeller geometry on the performance of semi-open ceramic centrifugal fan impellers at elevated temperatures. Exp Therm Fluid Sci 2005;30:565–77.
3. Engin T, Gur M. Performance characteristics of a centrifugal pump impeller with running tip clearance pumping solid-liquid mixtures. J Fluids Eng 2001;123:532–8.
4. Eum HJ, Kang YS, Kang SH. Tip clearance effect on through-flow and performance of a centrifugal compressor. KSME Int J 2004;18:979–89.
5. Nili-Ahmadabadi M, et al. Investigation of a centrifugal compressor and study of the area ratio and TIP clearance effects on performance. J Therm Sci 2008;17:314–23.
6. Rajakumar DR, Ramamurthy S, Govardhan M. Study on the performance deterioration of mixed flow impeller due to change in tip clearance. J Therm Sci 2013;22:532–8.
7. Hong SS, Abhari RS. Effect of tip clearance on impeller discharge flow and vaneless diffuser performance of a centrifugal compressor. Proc Instn Mech Engrs Part A 2012;226:963–74.
8. Ayder E, Van den Braembussche R, Brasz JJ. Experimental and theoretical analysis of the flow in a centrifugal compressor volute. J Turbomach 1993;115:582–9.
9. Jung Y, et al. Effects of a Nonuniform Tip clearance profile on the performance and flow field in a centrifugal compressor. Int J Rotat Mach 2012. ID 340439.
10. Engin T. Study of tip clearance effects in centrifugal fans with unshrouded impellers using computational fluid dynamics. Proc Instn Mech Engrs Part A 2006;220:599–610.
11. Asuaje M, et al. Numerical modelization of the flow in centrifugal pump volute influence in velocity and pressure fields. Int J Rotat Mach 2005;3:244–55.
12. Hariharan C, Govardhan M. Effect of inlet clearance gap on the performance of an industrial centrifugal blower with parallel wall volute. Int J Fluid Mach Syst 2013;6:113–20.
13. Hariharan C, Govardhan M. Loss in input power due to increase in clearance between inlet duct and impeller in an industrial centrifugal blower. 4th International Conference on Advances in Energy Research 2013; 1336.
14. Celik IB. Procedure for estimation and reporting of discretization error in CFD applications. J Fluids Eng 2008; 130:078001.
15. Rakesh Bhargava. Flow and optimisation studies on splitter vaned centrifugal impellers. M.S. Thesis. 1978; Indian Institute of Technology Madras.
16. Kim Y, Engeda A, Aungier R. The influence of inlet flow distortion on the performance of a centrifugal compressor and development of an improved inlet using numerical simulation. Proc Instn Mech Engrs 2001;215:323–38.